27th EPS Conference on Contr. Fusion and Plasma Phys. Budapest, 12-16 June 2000 ECA Vol. **24B** (2000) 532 -535

Characteristics of Global Confinement Properties in TPE-RX Reversed Field Pinch

Y. Yagi, T. Shimada, H. Sakakita, Y. Hirano, S. Sekine and H. Koguchi

Electrotechnical Laboratory, 1-1-4 Umezono, Tsukuba, Ibaraki 305-8568, Japan

Abstract

Global confinement properties in the TPE-RX, reversed-field pinch device, are estimated from the data obtained by Thomson scattering, a neutral particle energy analyzer and an interferometer. The *I/N* value (*I*, plasma current, and *N*, column density) is relatively high ($12x10^{14}$ Am) and comparable to that of forerunner medium-sized TPE machines of the same vessel materials. In spite of the high *I/N* value, poloidal beta and energy confinement time are comparable to those of similarly sized large reversed field pinch machines (RFX and MST) under normal operating conditions. Energy confinement time in TPE-RX ranges from 0.5 ms to 1 ms and has a weak dependence on plasma current. Confinement properties are comparable between the locked and nonlocked discharges in the current flat top phase. A pulsed poloidal current drive technique is attempted in TPE-RX and the result shows improvement of confinement properties by a factor of two. The result is compared with that of the shot-by-shot theta scan experiment.

1. Introduction

TPE-RX [1] is a large-sized reversed field pinch (RFP) machine with R/a = 1.72/0.45 m, where R and a are the major and minor radii, respectively. The machine is characterized by a close-fitting (b/a = 1.08, b being the minor radius of the innermost shell), multilayered conductive shell with equilibrium control by DC external field with the aid of a pulsed poloidal coil inside the thick shell that assists gas breakdown. The vacuum vessel is made of stainless-steel type 316L with fixed molybdenum limiters. TPE-RX aims at optimization and understanding of the confinement properties of RFP plasmas up to the designed maximum plasma current (I_p) of 1 MA. The maximum I_p and pulse duration time, τ_d, of 0.48 MA and 0.1 s have been attained, independently. Note that the maximum I_p is limited by the total energy of the capacitor bank system.

Recently, the diagnostics for the global confinement properties (using an interferometer for n_{el}, Thomson scattering for T_{e0} and n_{e0}, and a neutral particle energy analyzer (NPA) for T_i) have been brought into operation; here the variables have their usual meanings. In this paper we report the results of the first measurement of the global confinement properties of the RFP plasma in TPE-RX at I_p < 0.4 MA.

2. Confinement properties

First, it was confirmed by a statistical normalization technique that both electrons and ions have Maxwellian distribution functions without any noticeable tail components up to 3 keV at I_p = 0.35 MA. It was also confirmed that optimum confinement properties are obtained at t = 31 ms which is approximately the center of the current flat top phase. Then, I_p was scanned from 0.2 MA to 0.4 MA with the measurement of T_{e0}, n_{e0} and T_i at t = 31 ms. The I_p scanning experiment was conducted at the same filling pressure of deuterium gas, p_{D2} (= 0.7 mTorr) without using any active density control, and with the same Θ and F (Θ = 1.5, F = -0.15), where Θ and F are the pinch and reversal parameters, respectively. No external equilibrium control was applied since the equilibrium shift is negligible owing to the outward shift of the vacuum vessel with respect to the center of the thick shell.

Figure 1(a) shows that n_{el} linearly increases with I_p and I/N ($I = I_p$ and $N = \pi\langle n_e\rangle$, $\langle n_e \rangle$ is the volume averaged electron density) is relatively high ($12x10^{14}$ Am). The value of I/N in TPE-RX is exactly the same as those in forerunners, TPE-1RM20 (R/a = 0.75/0.192 m) and TPE-1RM15 (R/a = 0.70/0.137 m) which had the same materials for the vacuum vessel (stainless-steel type 316L with molybdenum limiters). It has been generally observed in RFP plasmas that the global confinement properties decrease with *I/N* [2, 3]. It is interesting to note that the poloidal beta, β_p, in TPE-RX (5-10%) is comparable to or even slightly better than the values extrapolated from the combined tendency versus *I/N* plots derived from [2, 3]. We will conduct an n_e-scan, independently of I_p, by means of the gas-puffing technique, in order to obtain a complete scaling database for comparison with other machines.

The energy confinement time, τ_E, vs. I_p is plotted in Fig. 1(b). It is assumed that $n_i = n_e$, T_i from NPA is the temperature at the plasma center, and the pressure profile is parabolic. Figure 1(b) shows that τ_E ranges from 0.5 ms to 1 ms, and shows some degradation at $I_p > 0.35$ MA. Generally, τ_E shows a weak dependence on I_p. More details are given in [4]. The best I_p-scaling of τ_E in RFP plasmas is predicted to scale as $\tau_E \sim I_p^{1.5}$ with a constant beta [5]. Namely, the result in Fig. 1 shows some deviation from the best-predicted scaling. The apparent weak dependence of τ_E on I_p can be explained by engineering factors, that stem from the means of operation and/or the plasma-wall interaction, and by the intrinsic nature of the RFP plasma in a machine of this size over the scanned range of I_p. Note that the former can be affected by the latter.

Concerning the engineering factors, we note here the increase in loop voltage, V_{loop}, with I_p and the degradation of T_{e0} at $I_p > 0.35$ MA. It is observed that V_{loop} increases almost linearly with I_p, while T_{e0} increases with I_p up to $I_p = 0.35$ MA. These can be attributed to either a change of the spatial profile of the plasma resistivity, an increase in Z_{eff}, or the existence and increase in the loop voltage anomaly term. The value of Z^* is estimated to be approximately 9 at $I_p = 0.3$ MA, which is estimated through the helicity balance equation by using Spitzer's resistivity with the measured T_{e0} and an assumption of the spatial profiles for T_e and Z_{eff}. Experimentally, measurement of the spatial profiles of Z_{eff} and T_e is necessary to conclude the existence of the loop voltage anomaly. A relatively high Z_{eff} is possible in the low-density plasma ($n_{el} = 0.5 \times 10^{19}$ m^{-3} at $I_p = 0.3$ MA), particularly in the vessel made from stainless-steel with fixed molybdenum limiters. Alternatively, it is also possible that the loop voltage anomaly term exists in the plasma with relatively high *I/N* values [6]. The increase in Z^* with I_p might be due to the operation without DC equilibrium control, either through the increase in Z_{eff} caused by the increase in the global plasma-wall interaction (PWI) or through the increase in the loop voltage anomaly term, as modeled in [7]. The degradation of T_{e0} at $I_p > 0.35$ MA with an ohmic input power, P_{in}, of 9.5 MW may be an enhanced level of impurity due to the increase in the global or local PWI. Note that a similar degradation was observed in TPE-1RM20 at $I_p > 0.17$ MA with $P_{in} = 2.7$ MA. The averaged heat load at each critical I_p value is

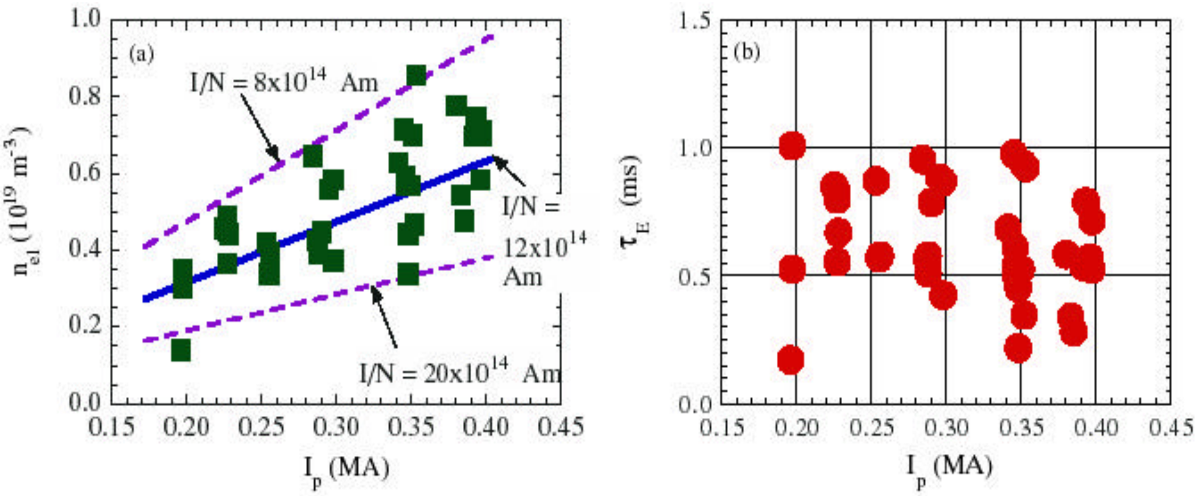

Figure 1. Plasma current dependece of the line averaged density, nel, (a) and energy confinement time, τE, (b) measured at t = 31 ms, pD2 = 0.7 mTorr, Θ = 1.5 and F = -0.15 in TPE-RX.

0.31 MW/m^2 and 16 kJ/m^2 (for 50 ms duration) in TPE-RX and 0.47 MW/m^2 and 4.7 kJ/m^2 (for 10 ms duration) in TPE-1RM20. The actual surface temperature of the first wall and the spatial locality of the PWI are important for further discussion. The observed increase in V_{loop} and the degradation of T_{e0} can be avoided by further optimizing the operating conditions and by wall conditioning using carbonization or bolonization techniques, which shall be experimentally conducted in the future to improve the confinement properties.

It is an important question whether the weak dependence of τ_E seen in Fig. 1 is caused by the intrinsic nature of the RFP plasma or not. The magnetic field fluctuation amplitude as a function of I_p, or more generally as a function of the Lundquist number, S, provides important information in terms of addressing this question. A recent study [8] showed a weak dependence of $\delta B_r/B_{pa}$ on S ($\sim S^{-0.2}$) for the locked mode amplitude which dominates MHD activities. A similar weak dependence on S ($S^{-0.2}$ for I/N = 6x10^{14} Am) is also observed in MST [9].

A local PWI can, in fact, be caused by the locked mode observed in TPE-RX [10]. An extensive examination of the experimental operating conditions has also revealed that there are discharges where the clear phase-locked structure disappears, particularly when the filling pressure is low (0.3-0.4 mTorr). We have recently made a comparison of the global confinement properties between the locked and nonlocked discharges which do not show spatially localized enhanced magnetic structure. The result shows that τ_E is comparable (~ 0.8 ms) at t = 31 ms at I_p = 0.25 MA. Most of the discharges exhibited the locked mode in the I_p-scan shown in Fig. 1. The deterioration at I_p > 0.35 MA might be related to the local PWI caused by the locked mode. However, it is confirmed that the global confinement properties at I_p < 0.25 MA are not affected by the existence of the locked mode as far as the confinement in the current flat top phase is concerned.

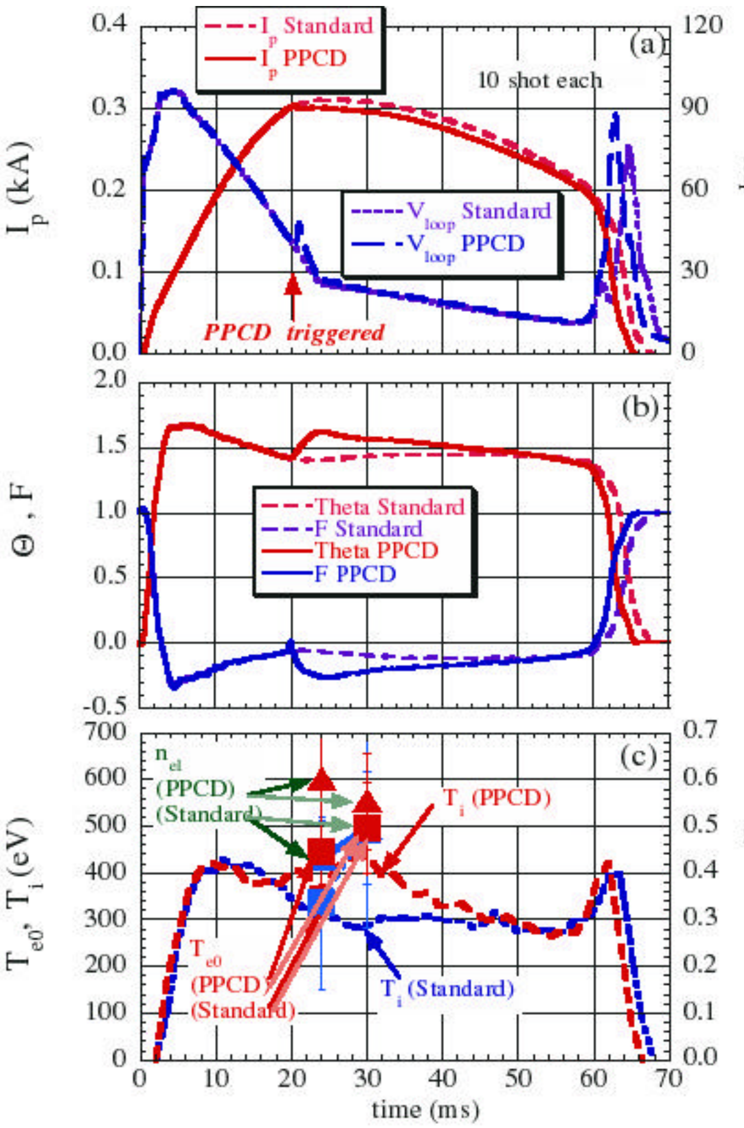

Figure 2. Comparison of the standard discharges and a single pulse PPCD experiment

3. PPCD

After the first measurement of the global confinement properties in TPE-RX under normal operating conditions, we moved on to conduct trials for the improved confinement regimes. We attempted a pulsed-poloidal current drive (PPCD) [11] and theta scan experiments. Figure 2 shows the shot-averaged waveforms in the standard discharges and in the PPCD discharges at I_p = 0.3 MA. The reversal bank is triggered at t = 20 ms to drive the toroidal magnetic field into a deeper reversal, thus inducing a poloidal electric field inside the plasma in such a way as to drive the poloidal current which is normally sustained by dynamo activity. Figure 2(a) shows that I_p and V_{loop} are almost the same while F and Θ, in Fig. 2(b), change transiently after triggering of PPCD. The intensity of the soft X-ray signal shows a sharp increase after the triggering of PPCD. Abrupt decrease in intensity of the soft X-ray signal is often observed immediately after the peak at t = 24 ms. Note that the penetration time of the toroidal field into the vacuum vessel is 2 ms. In some cases, however, the level of the soft X-ray signal is maintained at the level of its peak, if such a relaxation event does not occur. The increase in T_{e0}, n_{e0} and T_i is also confirmed in the PPCD discharges as shown in Fig. 2(c). T_i shows a slower increase than T_{e0} and n_e. The central plasma pressure, *p(0)*, shows an increase by a factor of 2 at the peak of the soft X-ray signal. The net input power, $P_{oh} = P_{in} - dW_m/dt$, shows a large oscillation for 10 ms after triggering of PPCD. The shot-averaged P_{oh} has a minimum at t = 22.5 ms. If we assume that the spatial profiles of T_e, T_i and n_e do not change due to PPCD, it is estimated that β_p and τ_E also increase by a factor of 2 at t = 24 ms.

In order to understand the improvement of the confinement in the PPCD discharge, the confinement properties were compared with those in the shot-by-shot theta scan experiment. This is to distinguish the beneficial nature of the transient characteristics of the PPCD discharge. The theta was scanned over a relatively limited range (Θ < 1.7). The shot-averaged trajectories are compared in Fig. 3 among the PPCD discharge and four discharges operated at different Θ values. It is seen that the trajectory in the PPCD moves from the line of F = 1-0.75Θ to F = 1-0.80Θ, while the steady-state theta scan follows the former line. This change is possible if $\tau_{PPCD} < \tau_{diff}(0)$, where $\tau_{PPCD} = (1/B_{tw}(dB_{tw}/dt))^{-1}$ and $\tau_{diff}(0)$ is the diffusion time of the core plasma. This condition might be important to drive the plasma into a more stable region for higher Θ plasmas which potentially can have higher β_p values.

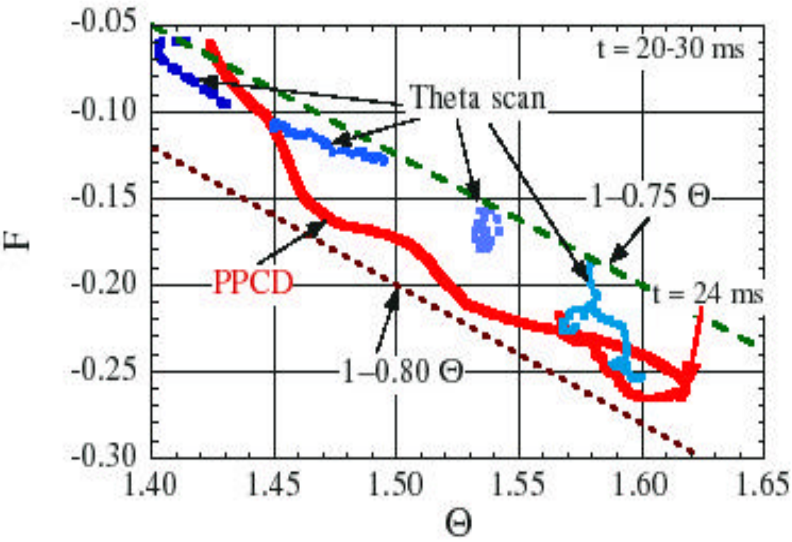

Figure 3. F-Theta trajectories of the shot-by-shot theta scan and the PPCD experiments

References

[1] Yagi Y et al, Fusion Eng. and Design **45** (1999) 409 and **45** (1999) 421.
[2] Hokin et al, Phys. Fluids **3** (1991) 2241.
[3] Antoni V et al, Proc. IAEA Seville, 1994, Vol. 2. (1995) p. 405.
[4] Yagi Y et al, submitted to Nucl. Fusion.
[5] Connor J W and Taylor J B, Phys. Fluids **27** (1984) 2676.
[6] Hedin G et al, Plasma Phys Control. Fusion **38** (1996) 657.
[7] Jarboe T R and Alper B, Phys. Fluids **30** (1987) 1177.
[8] Malmberg J A et al, submitted to Phys. of Plasmas.
[9] Fiksel G et al, Proc. IAEA Yokohama, 1998, Vol. 1 (1999) p. 383.
[10] Yagi Y et al, Phys. of Plasmas **6** (1999) 3824.
[11] Sarff J S et al, Phys. Rev. Lett. **72** (1994) 3670.